Detection of Nitrogen and Neon in the X-ray Spectrum of GP Com with *XMM/Newton*

Tod E. Strohmayer

Laboratory for High Energy Astrophysics, NASA's Goddard Space Flight Center, Greenbelt, MD 20771; stroh@clarence.gsfc.nasa.gov

ABSTRACT

We report on X-ray spectroscopic observations with *XMM/Newton* of the ultra-compact, double white dwarf binary, GP Com. With the Reflection Grating Spectrometers (RGS) we detect the Lα and Lβ lines of hydrogen-like nitrogen (N VII) and neon (Ne X), as well as the helium-like triplets (N VI and Ne IX) of these same elements. All the emission lines are unresolved. These are the first detections of X-ray emission lines from a double-degenerate, AM CVn system. We detect the resonance (r) and intercombination (i) lines of the N VI triplet, but not the forbidden (f) line. The implied line ratios for N VI, $R = f/i < 0.3$, and $G = (f + i)/r \approx 1$, combined with the strong resonance line are consistent with a dense, collision-dominated plasma. Both the RGS and EPIC/MOS spectra are well fit by emission from an optically thin thermal plasma with an emission measure (EM) $\propto (kT/6.5 \text{ keV})^{0.8}$ (model *cevmkl* in XSPEC). Helium, nitrogen, oxygen and neon are required to adequately model the spectrum, however, the inclusion of sulphur and iron further improves the fit, suggesting these elements may also be present at low abundance. We confirm in the X-rays the underabundance of both carbon and oxygen relative to nitrogen, first deduced from optical spectroscopy by Marsh et al. The average X-ray luminosity of $\approx 3 \times 10^{30}$ ergs s^{-1} implies a mass accretion rate $\dot{m} \approx 9 \times 10^{-13}$ $M_\odot$ yr^{-1}. The implied temperature and density of the emitting plasma, combined with the presence of narrow emission lines and the low $\dot{m}$ value, are consistent with production of the X-ray emission in an optically thin boundary layer just above the surface of the white dwarf.

Subject headings: Binaries: general - Stars: individual (GP Com) - Stars: white dwarfs - cataclysmic variables - X-rays: stars - X-rays: binaries

1. Introduction

The AM CVn stars are among the most compact binary systems known. Their optical spectra are dominated by broad helium lines seen in emission. The lines originate in an accretion disk formed by mass transfer from a degenerate helium dwarf onto the primary white dwarf. Their orbital periods range from about 10 minutes to 1 hour. They are natural laboratories for the study of poorly understood binary evolution processes, such as common envelope evolution. Moreover, the absence of hydrogen allows for the study of accretion disks dominated by helium. They may also be a significant channel for the production of Type Ia supernovae and neutron stars via accretion induced collapse (see Warner 1995 for a review of these systems).

GP Com is one of the better studied, nearby AM CVn systems. It has a 46.5 minute orbital period (Nather Robinson & Stover 1981), resides at a distance of ≈ 70 pc (Thorstensen 2003), and has been studied extensively in the optical and UV. Recently, Marsh (1999) and Morales-Rueda et al.(2003) have used optical and UV spectroscopy of the helium lines to probe the dynamics of the system in great detail. In addition to helium, nitrogen emission lines have been seen in the UV (Lambert & Slovak 1981), and optical (Marsh, Horne & Rosen 1991; Marsh et al. 1995). These observations identified a nitrogen overabundance–at the expense of carbon and oxygen–which can naturally be explained by CNO-cycle processing in the primary, followed by mixing of the nitrogen-rich material into the secondary during a common envelope phase (Marsh et al. 1991). Optical spectra also show weaker evidence of neon and magnesium lines (Marsh et al. 1991), and an apparent underabundance of heavy elements, such as iron and silicon, which may be consistent with its high proper motion and suggested halo origin (see Giclas, Burnham & Thomas 1961). A number of ultracompact systems with neutron star primaries also show apparent neon enrichment (see Juett & Chakrabarty 2003; Schulz et al. 2001).

Accretion onto the primary white dwarf should make such systems soft X-ray sources, and indeed, several have been detected in the X-ray band, including the prototype AM CVn, CR Boo, and GP Com (van Teeseling & Verbunt 1994; Ulla 1995; and Eracleous, Halpern & Patterson 1991). The X-ray flux from accreting, non-magnetic white dwarfs is thought to originate in a boundary layer that shocks and decelerates the Keplerian flow, allowing it to eventually settle on the white dwarf. Early work suggested that the boundary layer should be optically thick–radiating in the soft X-ray band and extreme UV–at mass accretion rates above $\dot{m} \approx 1.6 \times 10^{-10} M_\odot$ yr^{-1} (Pringle & Savonije 1979). At accretion rates much less than this the boundary layer should become more radially extended and optically thin, producing a harder X-ray spectrum. Aspects of this basic theoretical scenario have been confirmed by more recent calculations (see, for example, Patterson & Raymond 1985; Narayan & Popham

1993; Popham & Narayan 1995).

To date, however, X-ray observations of most AM CVn systems have been made at relatively low signal to noise levels and with only modest spectral resolution. Partly because of this it has been difficult to constrain detailed aspects of the accretion physics, for example, the density, temperature and rotational structure of the boundary layer remain largely uncertain. For example, ROSAT observations of GP Com found the source at a flux level of $\approx 1.2 \times 10^{-11}$ ergs cm^{-2} s^{-1} in the 0.2 - 2 keV band, and confirmed that it is variable. These ROSAT observations also found that the 0.2 - 2 keV spectrum cannot be described by a single temperature component (van Teeseling & Verbunt 1994), but detailed modelling of the spectrum was problematic due to the relatively poor statistics and the restricted bandpass. Moreover, certain aspects of the observations do not seem to fit neatly within the boundary layer model (see van Teeseling, Beuermann & Verbunt 1996).

In this Letter we summarize the results of recent, high signal to noise X-ray spectral measurements of GP Com with *XMM/Newton*. These data represent perhaps the best X-ray spectral measurements of an AM CVn system to date, and also show the first X-ray emission lines from such a system. In §2 we describe high resolution spectroscopy with the RGS as well as broad band spectral modeling using the EPIC/MOS data. In §3 we discuss the implications of the spectal data for the nature of the X-ray source in GP Com and AM CVn's in general. We conclude with a brief summary of our principle findings.

2. XMM Observations

XMM/Newton observed GP Com for 56.5 ksec beginning on January 3, 2001. The EPIC observations were done in imaging mode. We used version 5.4.1 of the XMM software (SAS) to analyze the data. GP Com was easily detected at the few counts s^{-1} level in the EPIC instruments. There were no other significant sources in the field of view. A lightcurve combining data from the PN and MOS detectors is shown in Figure 1, and confirms substantial X-ray variability, including several 2 to 4 minute flares during which the X-ray flux increased by factors of 2 - 3. Flaring has often been seen in the UV and optical, particularly in the helium emission lines (Marsh et al. 1995). We will present a detailed timing study of GP Com in a subsequent paper. We extracted spectra and produced response files for each of the instruments using the relevant SAS tools. For the purposes of this work we present results on only the total, phase-averaged spectrum. We will explore spectral, and orbital phase variability in a future study.

2.1. The RGS Spectrum

The spectrum extracted from both RGS instruments is shown in Figure 2 along with identifications for all the strongest line features. Since there are no line detections in the 2nd order, we only show the 1st order spectra. The strongest detected feature is the Lyα line of hydrogenic nitrogen (N VII) at 24.78 Å, but other lines of nitrogen are also present, including the Lyβ line as well as the helium-like triplet of N VI at ≈ 29Å. The only other signifcant line features are due to neon. The hydrogenic Lyα and Lyβ lines as well as the helium-like triplet are detected. Particularly striking is the absence of any strong carbon or oxygen lines in the spectrum.

We fit the observed line features using Lorentzian profiles with the widths fixed at the appropriate width of the RGS line spread function (LSF) for that wavelength (see den Herder et al. 2001; Pollock et al. 2003). All the hydrogenic lines are well fit with such a profile and are unresolved. Table 1 summarizes the salient properties of all the detected lines.

As is well known, the helium-like triplets can be used as probes of the plasma conditions where the lines are produced (see, for example, Gabriel & Jordan 1969; Porquet & Dubau 2000). The line flux ratios, $R = f/i$, and $G = (i+f)/r$, of the resonance (r), intercombination (i) and forbidden (f) transitions which make up the triplet are sensitive to the electron density and temperature of the plasma, respectively. For each triplet we fit a Lorentzian profile at the rest wavelength of each transition. In order to determine the line ratios, we fixed the wavelength and width of each line, but allowed the line fluxes to vary. The signal to noise ratio in both triplets is not particularly high, but the line ratios can at least be roughly estimated. The nitrogen triplet is better resolved than that of neon. The results of our fits are shown in Figure 3 (see also Table 1 for the measured line ratios). For the N VI triplet we detect the resonance and intercombination lines, but interestingly, not the forbidden line. The line ratios for N VI, $R = f/i < 0.3$, and $G = (f + i)/r \approx 1$, and the strong resonance line are consistent with formation in a dense, collision-dominated plasma (Porquet & Dubau 2000). For nitrogen, a strong UV radiation field can also decrease the strength of the forbidden line, mimicking a density effect, however, the line ratios from the neon triplet–which are much less sensitive to radiation field effects–are also consistent with a plasma at or near the critical density $n_c = 5.3 \times 10^9$ cm^{-3} for nitrogen.

2.2. Broadband Spectral Modelling: MOS spectra

We used XSPEC version 11.3 to fit the EPIC/MOS and RGS spectra with several collisional ionization equilibrium (CIE) plasma emission models. We found that multi-

temperature models fit the data significantly better than single temperature models. For example, the multi-temperature and variable abundance model *cevmkl* in XSPEC provides an excellent fit to the data from both the RGS and EPIC instruments (see Mewe, Gronenschild & van den Oord 1985; Mewe, Lemen & van den Oord 1986; Liedahl, Osterheld & Goldstein 1995). This model uses a power law in temperature to describe the emission measure distribution (EM), vis., EM $\propto (kT/kT_{max})^\gamma$, where kT_{max} and γ are the maximum temperature and power law index, respectively.

Although pile-up in the EPIC spectra is not a major problem, there is some evidence for modest pile-up in the PN spectra, so for the broad-band spectral modeling we focused on the MOS data only. Figure 4 shows our best fit to the EPIC/MOS data using the *cevmkl* model. The model fits the data well, with a minimum χ^2 of 1,005 for 1,045 degrees of freedom. Using the MOS data only, the best-fit emission measure distribution is characterized by $kT_{max} = 6.3 \pm 0.3$ keV, and $\gamma = 0.85 \pm 0.05$. The 0.3 - 10 keV fluxes are 4.7 and 5.3×10^{-12} ergs cm^{-2} s^{-1} in the MOS1 and MOS2, respectively. Taking the mean of these fluxes, we arrive at an average luminosity (at a distance of 70 pc) of 2.94×10^{30} ergs s^{-1} in the same band.

The elements which are strongly required by the *cevmkl* fit to the MOS data are helium, nitrogen, oxygen and neon, however, χ^2 additionally improves by 13.35 and 23.9 with the inclusion of iron and sulphur, respectively, suggesting these elements may also be present at low abundance. No other elements are required to fit the spectrum. Using this model we determined the abundances relative to the solar values tabulated by Anders & Grevesse (1989). The implied abundance ratios relative to oxygen, by number, are; N/O = 10.1 ± 2, Ne/O = 1.62 ± 0.33, He/O = $1,933 \pm 390$, Fe/O = 0.01 ± 0.0035, and S/O = 0.047 ± 0.012.

3. Discussion

The detection of nitrogen lines in the X-ray band provides additional confirmation of the overabundance of nitrogen relative to carbon and oxygen deduced from optical spectra (Marsh et al. 1991). The high nitrogen abundance likely reflects the operation of CNO-cycle thermonuclear processing in the primary (Marsh et al. 1991). We find a nitrogen to helium ratio, by number, of $\approx 4.5 \times 10^{-3}$, which is moderately higher than the value derived by Marsh et al. (1991) of 2.7×10^{-3} (see their Table 4). Our derived oxygen to helium ratio is, however, about a factor of 10 higher than they deduced from the optical. Although systematic modelling effects could be present, these results provide a suggestion that the X-ray emitting gas may have somewhat higher oxygen abundance than the accretion disk (which produces the optical emission lines). If the accretor were an oxygen-rich white dwarf,

and some of its matter is mixed with the accreted material in the turbulent boundary layer, then this could perhaps increase the oxygen abundance relative to the donor material.

Our derived Ne/O ratio of 1.62 indicates an overabundance of neon by a factor of about 11 compared to the solar value. Neon is a by-product of helium burning under a wide range of conditions (see, for example, Clayton 1983; Iben & Truran 1983). Modelling of the optical spectra suggests a modest neon enrichment of about 1.3 compared to solar abundances (Marsh et al. 1991). From the X-ray spectrum we find a Ne/He ratio of more than $4\times$ solar, higher than the optical value. This could be another indication that the composition of the X-ray emitting gas is different from that of the optical line emitting gas, and might be "contaminated" by material from the accretor.

Based on *Chandra* observations, neon enhancements have been suggested for several ultracompact neutron star binaries; 4U 1543-624 and 2S 0918-549 (Juett & Chakrabarty 2003), and 4U 1627-67 (Schulz et al. 2001). For 4U 1543-624, Juett & Chakrabarty (2003) deduced Ne/O ≈ 1.5, by number, from studies of absorption edges in *Chandra* high resolution spectra, however, these measurements can be influenced by the unknown ionization structure in the circumbinary material. Nevertheless, it seems plausible that some AM CVn's might share some of the same evolutionary history as the ultracompact neutron star binaries, however, an important difference would appear to be the nitrogen enrichment and corresponding oxygen deficit found in GP Com, that is not seen in the neutron star binaries. Thus, there must be some important differences in their evolutionary histories.

The X-ray flux measurements provide a means to estimate the mass accretion rate, $\dot{m}$, onto the white dwarf primary in GP Com. Assuming matter falls from the inner Lagrange point onto the primary, and that half the gravitational potential energy is dissipated in the accretion disk (in the UV and optical bands), the X-ray luminosity, L_x can be approximated as (see, for example, Nelemans, Yungelson & Portegies Zwart 2004),

$$L_x = \frac{1}{2}\frac{GM_1\dot{m}}{R}\left(1 - \frac{R}{R_{L_1}}\right) , \tag{1}$$

where M_1, R, R_{L_1}, and $\dot{m}$ are the primary mass, primary radius, the distance from the inner Lagrange point to the center of the accretor, and the mass accretion rate, respectively. Solving for $\dot{m}$, and inserting the measured X-ray luminosity for L_x gives,

$$\dot{m} = 3.48 \times 10^{-13}\frac{R_9}{(M_1/M_\odot)}\left(1 - \frac{R}{R_{L_1}}\right)^{-1} M_\odot \, \mathrm{yr}^{-1} , \tag{2}$$

where R_9 is the radius of the primary in units of 10^9 cm, and $R/R_{L_1} \approx 0.2$ for a system like GP Com. For a primary mass, $M_1 = 0.5M_\odot$ (Morales-Rueda et al. 2003) and $R_9 = 1$

(Zapolsky & Salpeter (1969) we obtain $\dot{m} \approx 8.7 \times 10^{-13}$ $M_\odot$ yr^{-1}, which is similar to the value estimated by Marsh et al. (1991) from the optical properties of the accretion disk.

This accretion rate is substantially lower than the critical rate above which one expects the boundary layer to be optically thick (Pringle & Savonije 1979; Narayan & Popham 1993). In such a case the emitting plasma should have a maximum temperature of the order of 10^8 K, which is similar to the peak temperature of ≈ 6.5 keV (7.5×10^7 K) deduced from the spectral modelling. The presence of *narrow* emission lines also supports the formation of the X-ray spectrum in a boundary layer. From the width of the strongest line feature, N VII Lyα, we can obtain an upper limit on the velocity dispersion of the emitting plasma of ≈ 250 km s^{-1} (3σ) (This includes both bulk and thermal motions). This indicates an origin in a region close to the white dwarf and not, for example, further out in the accretion disk, which would have much higher characteristic circular velocities. For example, if the white dwarf accretor was synchronized with the orbital motion, then its characteristic rotational velocity would be ≈ 23 km s^{-1}. Alternatively, to have a rotational speed equal to our 250 km s^{-1} limit, a white dwarf with a radius of 1×10^4 km would require a spin period of ≈ 250 seconds. Indeed, an upper limit to the Doppler (ie. thermal motion) line width for the nitrogen lines using the peak plasma temperature of ≈ 6.5 keV indicates a value close to the 250 km s^{-1} limit, which tends to support a slowly rotating, or perhaps synchronized white dwarf.

The XMM/Newton spectral measurements provide a detailed look at the physics of the boundary layer between the accretion disk and white dwarf in GP Com. Further comparisons with theoretical boundary layer models could provide interesting constraints on the temperature, density and rotational profiles of the boundary layer. Deeper X-ray spectra would provide better temperature and density constraints from the helium-like triplets, and likely more lines of less abundant species would be detected, allowing more precise constraints on the composition.

References

Anders E. & Grevesse N. 1989, Geochimica et Cosmochimica Acta 53, 197.

Beuermann, K., Thomas, H. -C., Reinsch, K., Schwope, A. D., Trumper, J. & Voges, W. 1999, A&A, 347, 47.

Clayton, D. D. 1983, "Principles of Stellar Evolution and Nucleosynthesis," (Univ. of Chicago Press: Chicago).

Eracleous, M., Halpern, J. & Patterson, J. 1991, ApJ, 382, 290.

den Herder, J. W. et al. 2001, A&A, 365, L7.

Gabriel, A. H. & Jordan, C. 1969, MNRAS, 145, 241.

Giclas, H. L., Burnham, R., Jr., & Thomas, N. G. 1961, Lowell Obs. Bull., 112, 61.

Iben, I. & Truran, J. W. 1978, ApJ, 220, 980.

Juett, A. M. & Chakrabarty, D. 2003, ApJ, 599, 498.

Lambert, D. L. & Slovak, M, H. 1981, PASP, 93, 477.

Liedahl, D.A., Osterheld, A.L., and Goldstein, W.H. 1995, ApJL, 438, 115

Marsh, T. R., Wood, J. H., Horne, K. & Lambert, D. 1995, MNRAS, 274, 452.

Marsh, T. R., Horne, K. & Rosen, S. 1991, ApJ, 366, 535.

Marsh, T. R. 1999, MNRAS, 304, 443.

Mewe, R., Gronenschild, E.H.B.M., & van den Oord, G.H.J. 1985, A&AS, 62, 197.

Mewe, R., Lemen, J.R., & van den Oord, G.H.J. 1986, A&AS, 65, 511.

Morales-Rueda, L. et al. 2003, A&A, 405 249,

Narayan, R. & Popham, R, G. 1993, Nature, 362, 820.

Nather, R. E., Robinson, E. L. & Stover, R. J. 1981, ApJ, 244, 269.

Nelemans, G., Yungelson, L. R., & Portegies Zwart, S. F. 2004, MNRAS, 349, 181.

Patterson, J. & Raymond, J. C. 1985, ApJ, 292, 535.

Pollock, A. M. T. et al. 2003, XMM Calibration Document, XMM-SOC-CAL-TN-0030 Issue 2, "Status of the RGS Calibration,"

Popham, R. G. & Narayan, R. 1995, ApJ, 442, 337.

Porquet, D. & Dubau, J. 2000, A&AS, 143, 495.

Pringle, J. E. & Savonije, G. J. 1979, MNRAS, 187, 777.

Schulz, N. S. et al. 2001, ApJ, 563, 941.

Thorstensen, J. R. 2003, AJ, 126, 3017.

Ulla, A. 1995, A&A, 301, 469.

van Teeseling, A. Beuermann, K. & Verbunt, F. 1996, A&A, 315, 467.

van Teeseling, A. & Verbunt, F. 1994, A&A, 292, 519.

Warner, B. 1995, *Cataclysmic Variable Stars*, Cambridge Univ. Press, Cambridge UK.

Zapolsky, H. S. & Salpeter, E. E. 1969, ApJ, 158, 809.

Figure Captions

Fig. 1.— A lightcurve of a portion of the *XMM/Newton* EPIC (PN+MOS) observation of GP Com. The binsize is 80 s. Significant variability is evident on a range of timescales. A characteristic error bar is also shown (upper left).

Fig. 2.— High resolution spectra of GP Com obtained with the RGS1 (bottom) and RGS2 (top) spectrometers in the $7 - 32$ Å band (solid histogram). Identifications are given for the prominent lines. The best fitting, variable emission measure plasma model (*cevmkl* in XSPEC) is also shown (solid curve).

Fig. 3.— RGS spectra and best fitting Lorentzian line profiles for the N VI (top) and Ne IX (bottom) helium-like triplets.

Fig. 4.— Phase-averaged spectrum of GP Com as observed in the EPIC/MOS detectors (MOS1:white, MOS2:red). Shown are the data and best fitting *cevmkl* model versus wavelength using XSPEC. The fit includes contributions from helium, nitrogen, oxygen, neon, sulphur and iron.
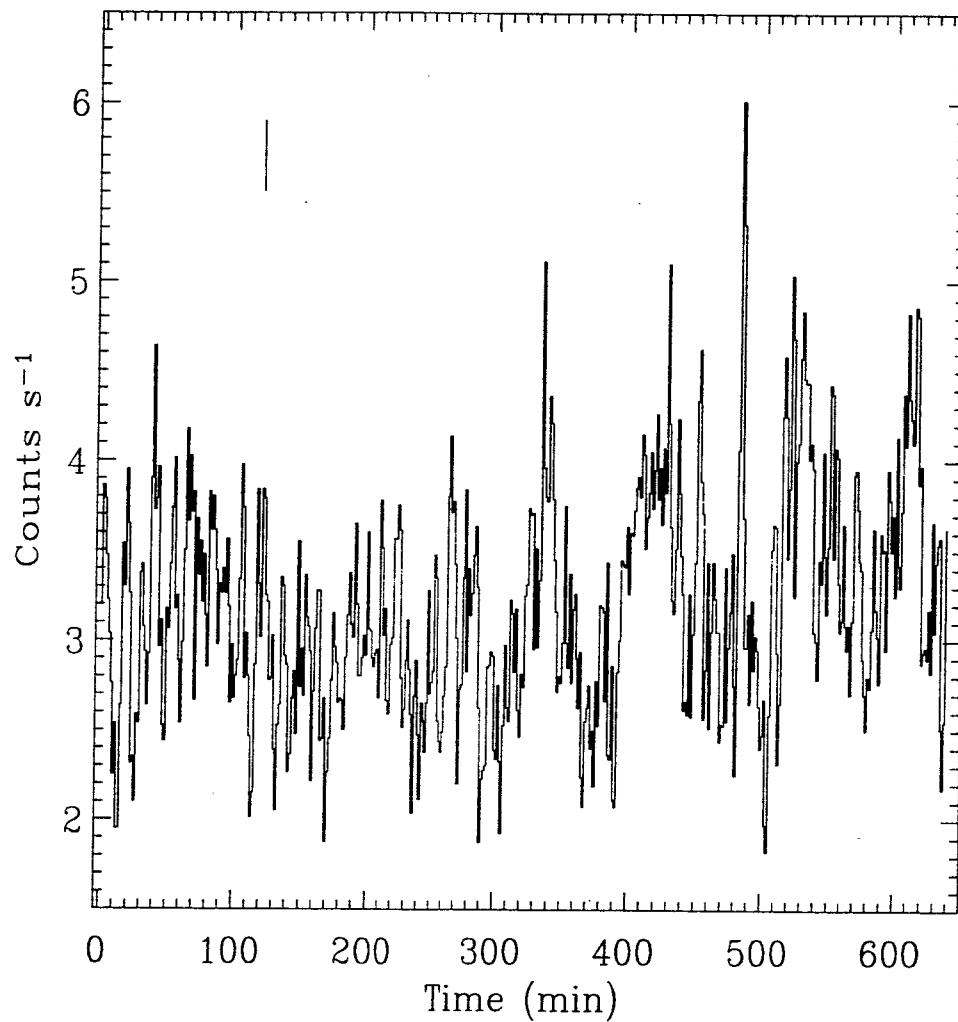
Figure 1: A lightcurve of a portion of the *XMM/Newton* EPIC (PN+MOS) observation of GP Com. The binsize is 80 s. Significant variability is evident on a range of timescales. A characteristic error bar is also shown (upper left).
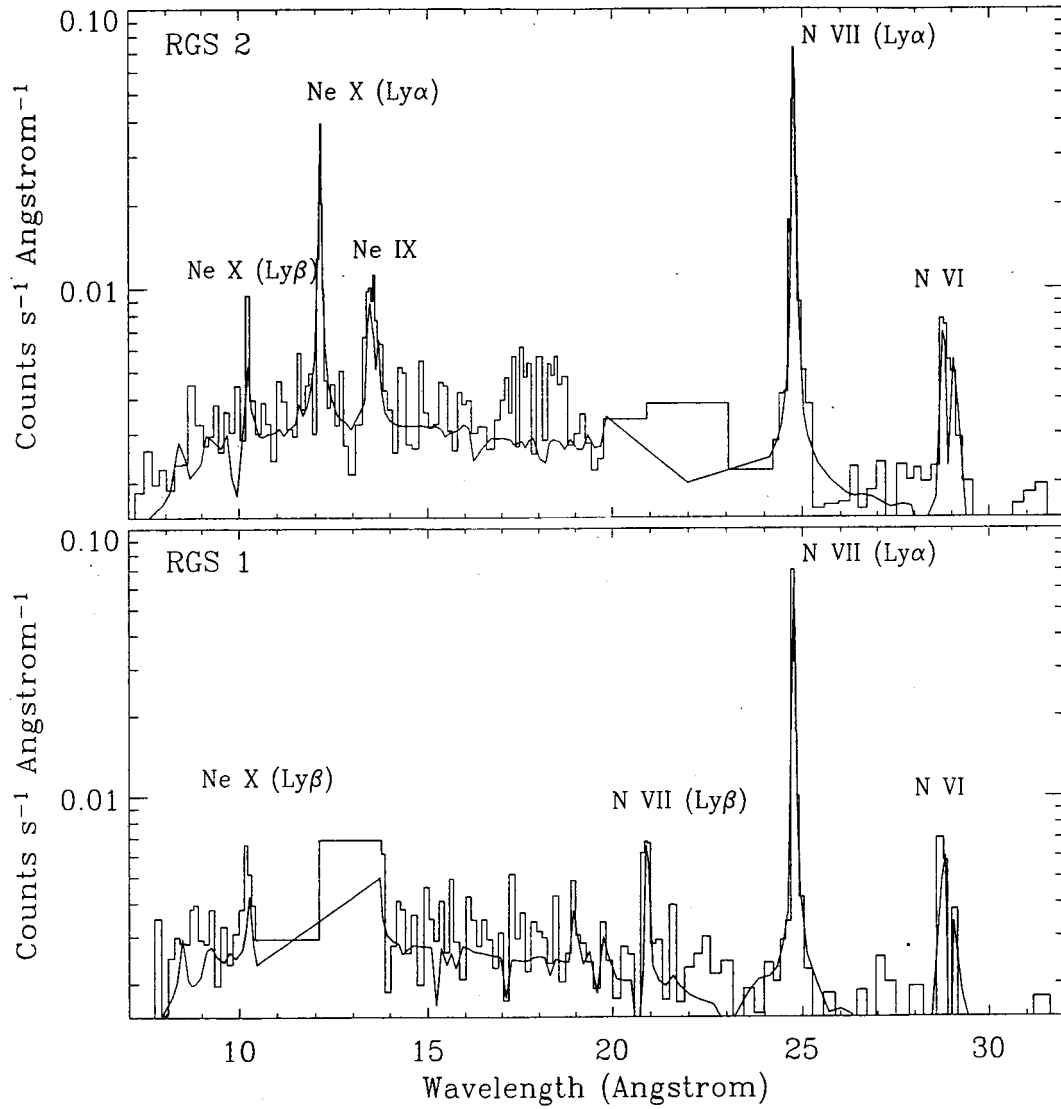
Figure 2: High resolution spectra of GP Com obtained with the RGS1 (bottom) and RGS2 (top) spectrometers in the $7 - 32$ Å band (solid histogram). Identifications are given for the prominent lines. The best fitting, variable emission measure plasma model (cevmkl in XSPEC) is also shown (solid curve).
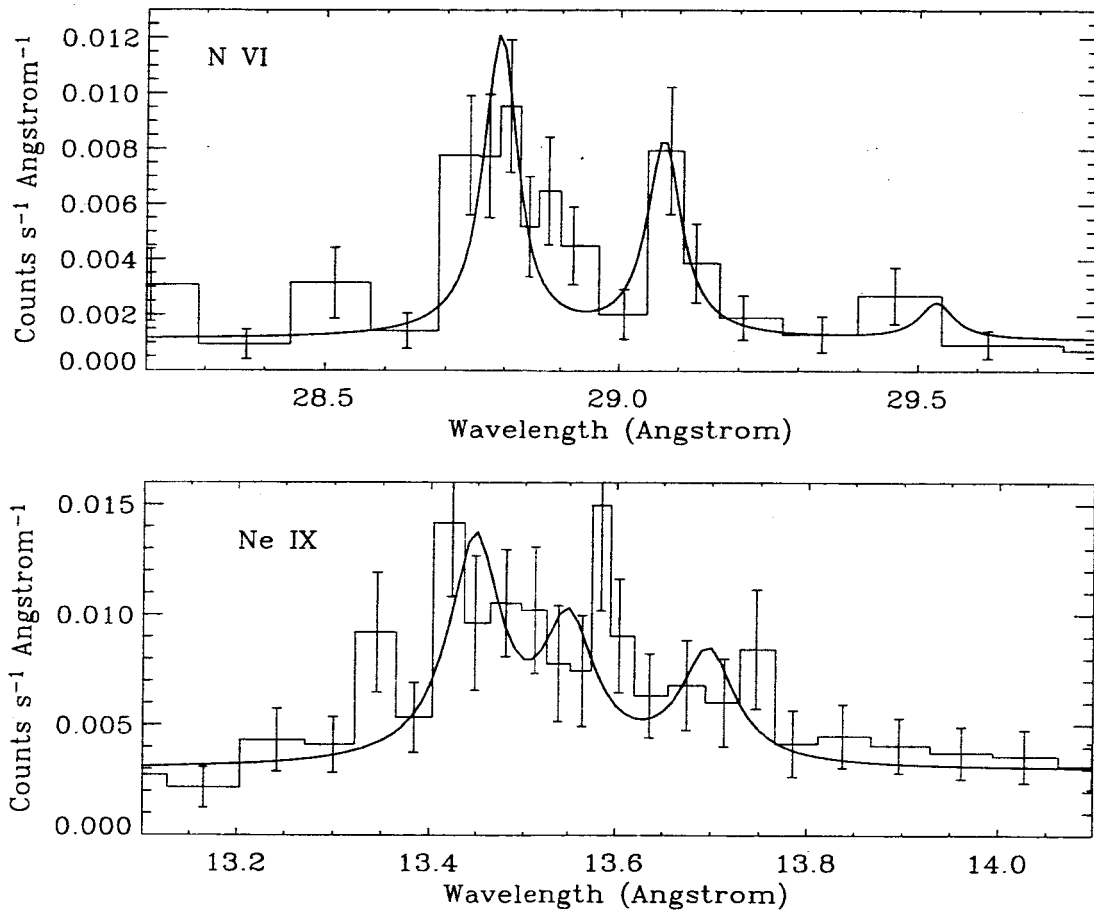
Figure 3: RGS spectra and best fitting Lorentzian line profiles for the N VI (top) and Ne IX (bottom) helium-like triplets.
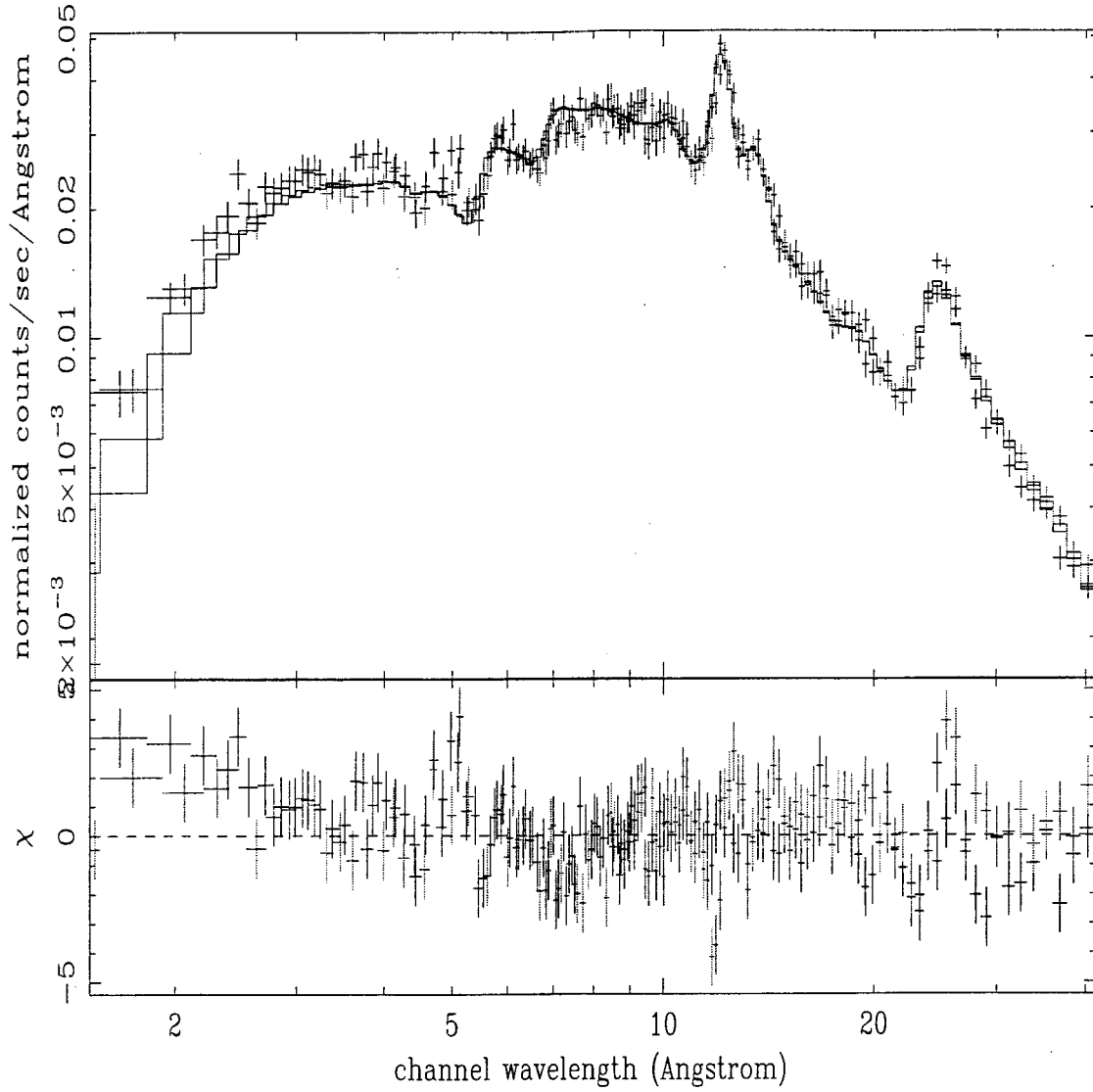
Figure 4: Phase-averaged spectrum of GP Com as observed in the EPIC/MOS detectors (MOS1:white, MOS2:red). Shown are the data and best fitting *cevmkl* model versus wavelength using XSPEC. The fit includes contributions from helium, nitrogen, oxygen, neon, sulphur and iron.

Table 1: Emission Line Properties for GP Com

Species	λ ($\mathring{A}$)				Flux	
	r	i	f		(10^{-4} cm^{-2} s^{-1})	
N VII		24.781			1.86	
N VII		20.910			0.28	
N VI	28.792	29.075	29.531	0.34	0.22	0.07[1]
Ne X		12.134			0.54	
Ne X		10.239			0.16	
Ne IX	13.447	13.550	13.697	0.20	0.11	0.09

[1] Not detected. 1σ upper limit.